Second Order Semi-Lagrangian Algorithms for the Study of Hydrodynamics of Electrochemical Cells

Eberson Luis de Souza Moraes, ebersonsm@yahoo.com.br

Metallurgy and Materials Engineering Department – Federal University of Rio de Janeiro, PO Box 68505, 21941-972 Rio de Janeiro, RJ, Brazil

Gustavo Charles Peixoto de Oliveira, tavolesliv@gmail.com

Group of Environmental Studies for Water Reservatories – GESAR/State University of Rio de Janeiro, Rua Fonseca Telles 524, 20550-013, Rio de Janeiro, RJ, Brazil

Gustavo Rabello dos Anjos, gustavo.rabello@gmail.com

Group of Environmental Studies for Water Reservatories – GESAR/State University of Rio de Janeiro, Rua Fonseca Telles 524, 20550-013, Rio de Janeiro, RJ, Brazil

Norberto Mangiavacchi, norberto.mangiavacchi@gmail.com

Group of Environmental Studies for Water Reservatories – GESAR/State University of Rio de Janeiro, Rua Fonseca Telles 524, 20550-013, Rio de Janeiro, RJ, Brazil

José Pontes, jopontes@metalmat.ufrj.br

Metallurgy and Materials Engineering Department – Federal University of Rio de Janeiro, PO Box 68505, 21941-972 Rio de Janeiro, RJ, Brazil

Abstract. *Proceeding with previous works made by Dos Anjos (2007) and Oliveira (2011) in their M.Sc. Dissertations, developed in the Metalurgy and Materials Graduate Program of the Instituto Alberto Luiz Coimbra (COPPE – Brazil), this work deals with the introduction of new features in a FEM – Finite Element Method code originally written by those authors, for the study of the hydrodynamic stability in electrochemical cells with rotating disk electrode A review of the related bibliography and the relevance of the subject can be found on the two cited M.Sc. Dissertations.*
Currently, the FEM Code developed in our group features a first order in time semi-Lagrangean scheme for interpolation of the shape functions for MINI elements. On a first step, QUADRATIC elements is now implemented, for discretization of the spatial domain. The following step, not yet implementd, will cope with the implementation of a second order in time semi-Lagrangea scheme. It is expected that both features will improve the precision of the results obtained with the code.
Keywords: *Corrosion, Rotating Disk Flow, Second-Order Algorithms, Semi-Lagrangian Method, Finite Element Method*

1. INTRODUCTION

The problem of current oscillations in electrochemical cells using a rotating disk electrode has been addressed for more than 15 years by the Metallurgy and Materials Engineering Department of the Federal University of Rio de Janeiro. The electrochemical system herein considered basically comprises a cell with a rotating disk working electrode driven by a variable velocity electric motor, a reference electrode and a counter electrode consisting of a platinum screen close to the cell sidewalls. The electrolyte consists of a $1 M H_2SO_4$ solution. Fig. 1 schematically shows the system setup.

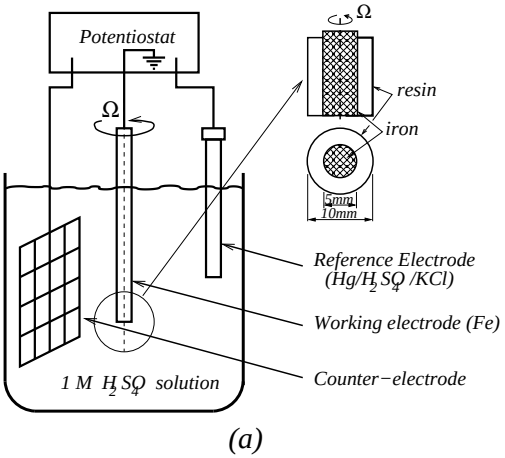

(a)

Figure 1. A scheme of typical setup of electrochemical cells with rotating disk electrodes

Stability analysis of the flow induced by the rotating disk electrode reinforces the hypothesis that the current oscillations originate from a hydrodynamic instability of the flow, boosted by the coupling of the hydrodynamics with the concentration field generated by dissolution of the iron electrode in the electrolyte Pontes *et al.* (2004), Mangiavacchi *et al.* (2007). A base state consisting of a generaliza-

tion of von Kármán's classical solution for rotating disk flow becomes unstable for Reynolds numbers beyond a certain treshold, leading to a spectrum of possible patterns including concentric circles, radial straight lines, logarithmic spirals, or a combination of these basic ones. The emerging patterns superpose to base state. Study of the transition to a more structured state finds applications not only in electrochemistry, but also in high speed aerodynamics, in pattern formation of turning agregates in cosmology and in the dynamics of turning fluid media in general.

Fig. 2 schematically shows the solution by von Kármán and Angew (1921) solution for rotating disk flow where the axial, radial and azimuthal components of the velocity can be observed, in cylindrical coordinates. The magnitude of the velocity components depends on the angular velocity imposed to the electrode and on the viscosity of the fluid, in addition to the point considered. The radial flow is balanced by the axial incoming radial flow, matching the continuity requirement.

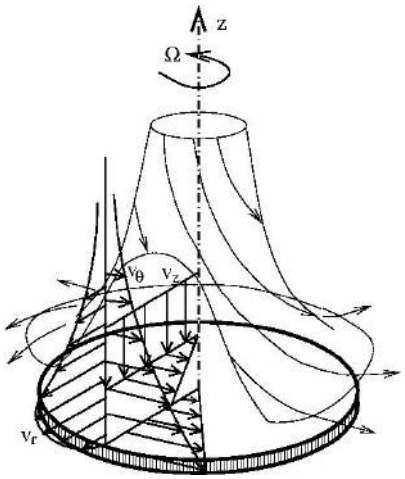

Figure 2. A scheme of von Kármán's flow close to a rotating disk.

The results from the linear stability analysis motivated our group to pursue the analysis of the hydrodynamics of electrochemical cells by solving the coupled hydrodynamic and chemical species transport equations using the Finite Element Method (FEM). First results for the steady coupled fields were obtained by Dos Anjos (2007), who developed a FEM code featuring three possible electrolyte configurations: constant viscosity, electrolyte viscosity depending on the axial coordinate and viscosity depending on the local concentration of ions originated from the dissolution of the iron electrode. In this case, the variable viscosity couples the hydrodynamic and the mass transport equations. Domain discretization is carried out using the *MINI element*, as shown in Fig. 3, and the material derivative is represented by a Semi-Lagrangian algorithm of first order.

2. GOVERNING EQUATIONS

$$\frac{D\mathbf{v}}{Dt} = -\frac{1}{\rho}\nabla p + \frac{1}{Re}\nabla\cdot\left[\nu\left(\nabla\mathbf{v} + \nabla\mathbf{v}^T\right)\right] \tag{1}$$

$$\nabla\cdot\mathbf{v} = 0 \tag{2}$$

$$\frac{Dc}{Dt} = \frac{1}{ReSc}\nabla\cdot(D\nabla c). \tag{3}$$

In the above equations, c is the concentration of the chemical species resulting from the dissolution of the iron electrode in the electrolyte, D is the diffusion coefficient of the species, Re and Sc are the Reynolds and Schmidt numbers, respectively.

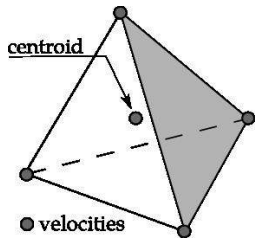

Figure 3. The mini-element adopted in the FEM code.

3. FINITE ELEMENT METHOD

In brief, we can mention that in the 1950's of last century, the finite element method was been widely used in the field of solid mechanics. With the consolidation of the *Galerkin method* for diffusion equations, in the 1970's, successful efforts were made to extend the method for fluid dynamics problems. Soon after, specific methodologies like *Petrov-Galerkin methods*, generalized Heinrich *et al.* (1977), Hughes *et al.* (1986), Johnson (1987), adaptive methods by Oden *et al.* (1989), Taylor-Galerkin method by Donea (1984), Lohner *et al.* (1985), discontinuous Galerkin method Oden *et al.* (1998), etc., were developed.

The finite element method is a general discretization procedure supported by ongoing problems statements defined mathematically. This reasoning strategy shows a consistent pattern with very useful computational methods for modern engineering. In this section, a short description of the variational formulation (or form) of the Navier-Stokes equations is presented, along with the semi-discrete Galerkin method (discretization of PDEs) and the semi-Lagrangian method.

3.1 Variational Formulation

The variational formulation is obtained by properly weighting the governing equations, namely, Eqs.(1)-(3). We obtain:

$$\int_\Omega \frac{D\mathbf{v}}{Dt}\cdot\mathbf{w}\,d\Omega - \frac{1}{\rho}\int_\Omega p\left[\nabla\cdot\mathbf{w}\right]\,d\Omega + \frac{1}{Re}\int_\Omega\left[\nu\left(\nabla\mathbf{v}+\nabla\mathbf{v}^T\right)\right]:\nabla\mathbf{w}^T\,d\Omega = 0 \tag{4}$$

$$\int_\Omega\left[\nabla\cdot\mathbf{v}\right]q\,d\Omega = 0 \tag{5}$$

$$\int_\Omega \frac{Dc}{Dt}r\,d\Omega + \frac{1}{ReSc}\int_\Omega (D\nabla c)\nabla r^T\,d\Omega = 0. \tag{6}$$

Functions $\mathbf{w}$, q and r are the *weighting functions* defined in the space $\mathcal{V}$ with the prescription: $\mathcal{V} := \left\{\mathbf{w}\in\mathcal{H}^1(\Omega)\ \mid\ \mathbf{w}=0\ \text{in}\ \mathbf{V}_c\right\}$, where $\mathbf{u}_c$ is the *essential boundary condition* value, $\mathbf{V}_c$ a possible boundary for the domain Ω, $\mathcal{H}^1(\Omega) := \left\{\mathbf{u}\in\mathcal{L}^2(\Omega)\middle|\frac{\partial\mathbf{u}}{\partial x_i}\in\mathcal{L}^2(\Omega), i=1,\ldots,n\right\}$ and $\mathcal{L}^2(\Omega)$ is the *Lebesgue space*, i. e., the space of all *square integrable* functions.

3.2 The Semi-Discrete Galerkin Method

The semi-discrete Galerkin Method provides a partial discretization where the functions that approximate a solution for the governing equations (Eqs.(4)-(6)) comprise a linear combination of shape functions depending on the time and functions intended to depend on the space coordinates. Following this procedure we denote by NV, NP and NC the number of velocity, pressure and concentration nodes, respectively, of the discrete grid of elements of the original domain Ω. The following semi-discrete approximation functions are obtained:

$$\begin{aligned} v_x(\mathbf{x},t) &\approx \sum_{i=1}^{NV} u_i(t)N_i(\mathbf{x}) & v_y(\mathbf{x},t) &\approx \sum_{i=1}^{NV} v_i(t)N_i(\mathbf{x}) \\ v_z(\mathbf{x},t) &\approx \sum_{i=1}^{NV} w_i(t)N_i(\mathbf{x}) & p(\mathbf{x},t) &\approx \sum_{i=1}^{NP} p_i(t)P_i(\mathbf{x}) \\ c(\mathbf{x},t) &\approx \sum_{i=1}^{NC} c_i(t)C_i(\mathbf{x}) \end{aligned}$$

where the coefficients u_i, v_i, w_i, p_i e c_i denote continuous functions in the time (t) and functions $N_i(\mathbf{x})$, $P_i(\mathbf{x})$ and $C_i(\mathbf{x})$ are interpolation functions at specified positions $\mathbf{x}$ for the velocity, pressure and concentration, respectively.

The discretized system becomes, in matrix form:

$$\begin{aligned} \mathbf{M}\dot{\mathbf{a}} + \frac{1}{Re}\mathbf{K}\mathbf{a} - \mathbf{C}\mathbf{p} &= 0 \\ \mathbf{D}\mathbf{a} &= 0 \\ \mathbf{M_c}\dot{\mathbf{c}} + \frac{1}{ReSc}\mathbf{K_c}\mathbf{c} &= 0, \end{aligned}$$

where $\mathbf{M}$, $\mathbf{K}$, $\mathbf{C}$, $\mathbf{D}$, $\mathbf{M_c}$, $\mathbf{K_c}$, are matrices and $\mathbf{a}$, $\mathbf{c}$, $\dot{\mathbf{a}}$, $\dot{\mathbf{c}}$ vectors built from *Assembly* operator , given by $\mathcal{A}_{e=1}^{n_{el}}$, where n_{el} is the number of elements.

3.3 The semi-Lagrangian method

The use of a discrete representation of the substantial derivative in the discretized weak form of the governing equations can be observed. In this section we apply the semi-Lagrangian method to the substantial derivatives of the governing

equations, we obtain we obtain that holds for every scalar or vetorial field:

$$\frac{D\mathbf{v}}{Dt} = \frac{\mathbf{v}_i^{n+1} - \mathbf{v}_d^n}{\Delta t} \tag{7}$$

The global matrix system takes the following discrete form:

$$\mathbf{M}\left(\frac{\mathbf{v}_i^{n+1} - \mathbf{v}_d^n}{\Delta t}\right) + \frac{1}{Re}\mathbf{K}\mathbf{v}^{n+1} - \mathbf{C}p^{n+1} = 0 \tag{8}$$

$$\mathbf{D}\mathbf{v}^{n+1} = 0 \tag{9}$$

$$\mathbf{M}_c\left(\frac{c_i^{n+1} - c_d^n}{\Delta t}\right) + \frac{1}{ReSc}\mathbf{K}_c c^{n+1} = 0, \tag{10}$$

where $\mathrm{v}_d^n = \mathrm{v}^n(\mathbf{x}_d, t^n)$, $c_d^n = c^n(\mathbf{x}_d, t^n)$ and $\mathbf{x}_d$ refers to the starting point in the time $t^n \leq t \leq t^{n+1}$ with initial condition $\mathbf{x}(t^{n+1}) = \mathbf{x}_i$.

4. FIRST RESULTS

The FEM Code written by Dos Anjos (2007) and Oliveira (2011) features a domain discretization employing the MINI element. In this section we present first results obtained with the QUADRATIC element, including the axial profiles of the relevant variables of the problem.

4.1 The Numerical Grid

A computational grid assuming a finite cylindrical domain with rigid side and bottom walls was adopted. The rotating disk consists of a circular region on the top of the domain, turning with specified angular velocity. Beyond the radius of the rotating disk we assumed a flat surface on the domain upper surface, subjected to a specified pressure set to zero.

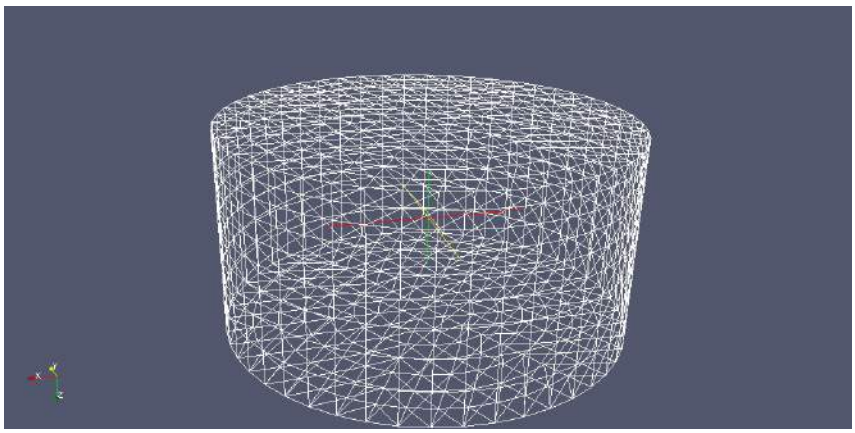

Figure 4. The numerical grid used in the simulations

4.2 Changes Introduced in the FEM Code

Two modifications were introduced in the FEM Code:

1. A new command was added to the code *Makefile* to select the element type;
2. The number of velocity nodes in each element was changed from 5 (MINI element) to 10 (QUADRATIC element) in the header file *TElement.h*, which defines the number of element nodes for each variable.

4.3 Numerical Simulations

After introducing the above changes in the code, some simulations were made in order to compare the results obtained with the use of the MINI element and with those obtained with the QUADRATIC element. Fig. 5 compares results obtained the two types of elements after 10, 200 and 800 time steps, respectively. A grid with the inner horizontal polygon with 6 sides, 8 polygons along the axial direction and 10 points along the axial direction was adopted.

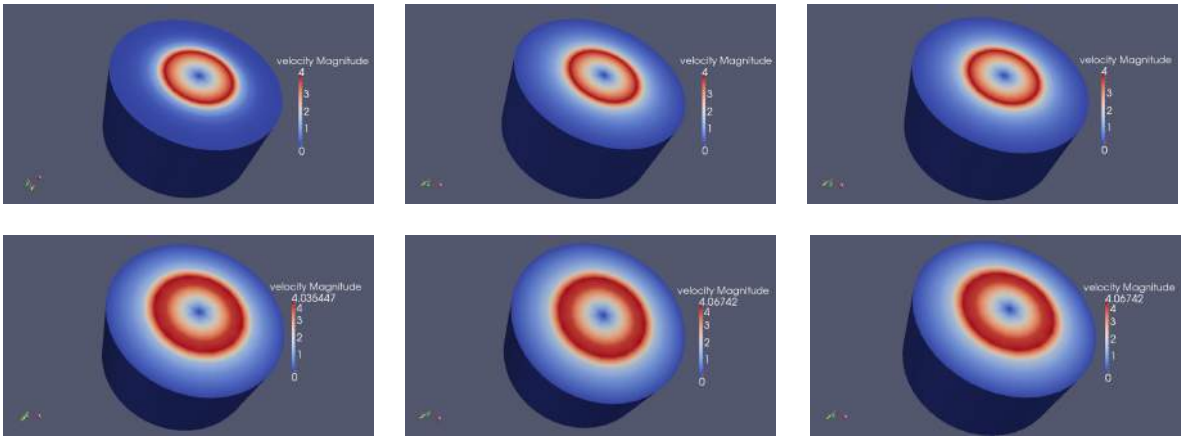

Figure 5. First line: Simulation with the MINI element after 10, 200 and 800 time steps, respectively. Second line: Simulation with the QUADRATIC element after 10, 200 and 800 time steps, respectively.

4.4 Comparing the Results Obtained with the Two Types of Elements

The simulations made with the two types of elements and presented in Fig. 6 show that the use of QUADRATIC elements leads to smoother and thus, more precise profiles than those obtained with the MINi element.

Fig. 6 compares the nondimensional velocity profiles at the upper surface of the domain in the 10^{th} time step of the simulation. The abscissæaxis refers to the radial coordinate at domain upper surface and the ordinate axis contains the velocity magnitude. F, G and H are defined as:

$$F = \frac{v_r}{r\Omega} \qquad G = \frac{v_\theta}{r\Omega} \qquad H = \frac{v_z}{(\nu\Omega)^{1/2}}, \tag{11}$$

where ν and Ω are the fluid viscosity and the disk angular velocity, respectively.

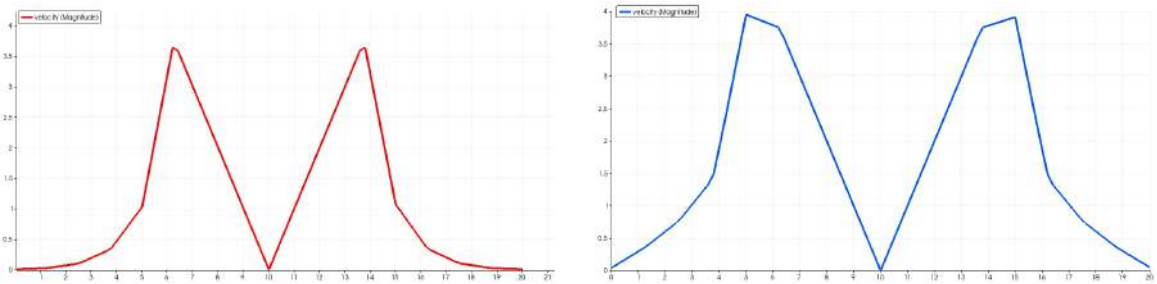

Figure 6. A comparison between the nondimensional velocity profiles at the rotating disk surface using the MINI element (left) and the QUADRATIC (right), after 10 time steps.

Fig. 7 compares the pressure profiles at the disk surface with the two types of elements in the 10^{th} time step of the simulation. Graphic axis are as above.

Figure 8 compares the nodimensional velocity profiles obtained with the two types of elements. Profiles identified

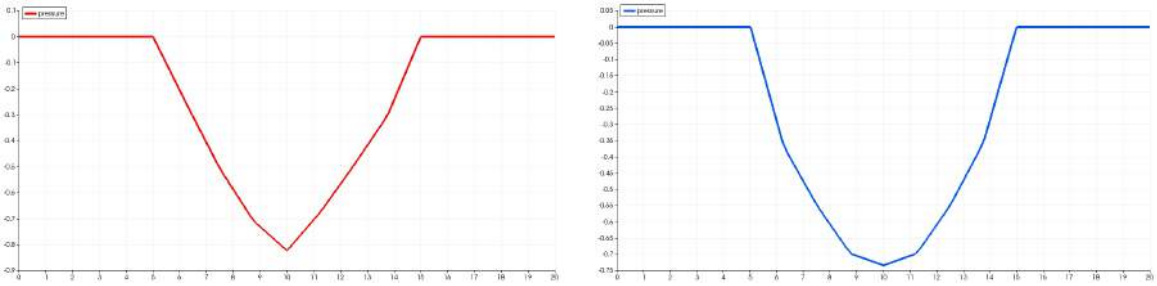

Figure 7. A comparison between the pressure profile at the rotating disk surface using the MINI element (left) and the QUADRATIC (right), after 10 time steps.

with a prime were obtained with the QUADRATIC element. The profiles are evaluated at the fourth point along the radial direction in the 10^{th} time step of the simulation.

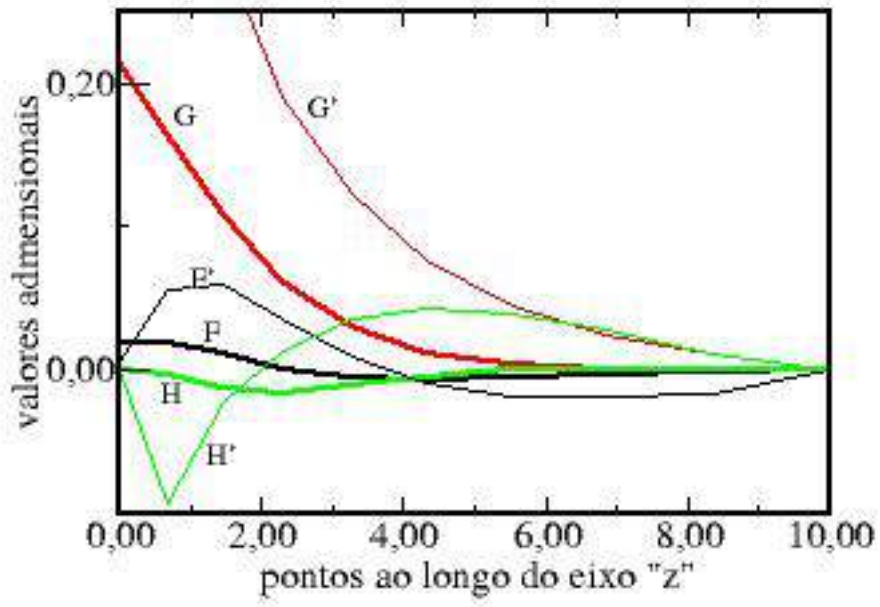

Figure 8. A comparison between the nondimensional velocity profiles with F, G and H, obtained with the two types of elements in the 10^{th} time step of the simulation.

From Fig. 8 we can see that simulations made with the QUADRATIC element result in more precise profiles.

5. REFERENCES

Donea, J., 1984. "A taylor-galerkin method for convective transport problems". *Int. J. Num. Methods Eng.*, Vol. 20, pp. 101–119.

Dos Anjos, G.R., 2007. *Solução do Campo Hidrodinâmico em Células Eletroquímicas pelo Método dos Elementos Finitos*. M.Sc. dissertation, COOPE/UFRJ, Rio de Janeiro, RJ, Brasil.

Heinrich, J.C., Huyakorn, P.S., Zienkiewiez, O.C. and Mitchell, A.R., 1977. "An upwind finite element scheme for two-dimensional convective transport equation". *Int. J. Num. Meth. Eng.*, Vol. 1, pp. 131–144.

Hughes, T., Franca, L. and Mallet, M., 1986. "A new finite element formulation for computational fluid dynamics: I. symetric forms of the compressible euler and navier-stokes euqation and the second law of thermodynamics". *Comp.*

Meth. Appl. Mech. Eng., Vol. 54, pp. 223–234.

Johnson, C., 1987. *Numerical Solution of Partial Differential Equations on the Finite Element Method*. Lund, Sweden, 1st edition.

Kármán, T.V. and Angew, Z., 1921. "Uber laminare and turbulente reibung". *ZAMM*, Vol. 1, pp. 233–252.

Lohner, R., Morgan, K. and Zienkiewiez, O.C., 1985. "An adaptive finite element procedure for compressible high speed flows". *Comp. Meth. Appl. Mech. Eng.*, Vol. 51, pp. 441–465.

Mangiavacchi, N., Pontes, J. and Barcia, O.E., 2007. "Rotating-disk flow stability in electrochemical cells: Effect of the transport of a chemical species". *Physics of Fluids*, Vol. 19, pp. 114–119.

Oden, J.T., Babuska, I. and Baumann, C.E., 1998. "A discontinuous hp finite element method for diffusion problems". *J. Comp. Phys.*, Vol. 146, pp. 491–519.

Oden, J.T., Demkowicz, L., Rachowicz, W. and Westerman, T.A., 1989. "Toward a universal h-p adaptive finite element strategy, part 2: A posterior error estimation". *Comp. Meth. Appl. Mech. Eng.*, Vol. 77, pp. 113–180.

Oliveira, G.C.P., 2011. *Estabilidade Hidrodinâmica em Células Eletroquímicas pelo Método de Elementos Finitos*. M.Sc. dissertation, COOPE/UFRJ, Rio de Janeiro, RJ, Brasil.

Pontes, J., Mangiavacchi, N. and Conceição, A.R., 2004. "Rotating-disk flow stability in electrochemical cells: Effect of viscosity stratification". *Physics of Fluids*, Vol. 16, pp. 707–716.

6. RESPONSIBILITY NOTICE

The authors is the only responsible for the printed material included in this paper.